Check for updates
Natural Product Sciences
32(1) : 93-103 (2026)
https://doi.org/10.20307/nps.2026.32.1.93

Phytochemical Investigation and Docking Study of Antidiabetic Compounds from The Methanol Extract of *Ceiba pentandra* (Bombacaceae)

Nadege Nelly Jounda[1], Samuel Magloire Bissim[4,*], Armel Junior Mbock[3], Mathieu Jules Tjegbe Mbenga[5], Claudine Ngueng[2], and Achille Nouga Bissoue[1,2,*]

[1]*Process Engineering Laboratory, Department of Chemical Engineering, HTTTC, University of Douala, Douala, Cameroon*
[2]*Chemistry Laboratory, Department of Chemistry, Faculty of Science, University of Douala, Douala, Cameroon*
[3]*Biology and Physiology Laboratory, Department of Animal Organism, Faculty of Science, University of Douala, Douala, Cameroon*
[4]*Chemistry Laboratory, Faculty of Science, University of Bamenda BP: 039, Bambili, Cameroon*
[5]*Centre for Drug Discovery, Faculty of Science, University of Buea, Buea, Cameroon*

Abstract – The bioactivity-guided isolation of hypoglycemic compounds from the crude methanolic root extract of *C. pentandra* led to the structural characterization of ten known compounds. Five of these compounds aridanin (**1**), corosolic acid (**2**), α-amyrin (**3**), (*E*)-methylsuberenol (**6**), and octadecanoic acid (**10**) were isolated from this genus for the first time, along with other known compounds: two flavonoids (quercetin (**4**) and kaempferol (**5**)), and three sterols (β-sitosterol (**7**), and stigmasterol (**8**) mixture), and β-sitosterol glucoside (**9**)). By using spectroscopic and spectrometric experiments, the isolated compounds were fully characterized by comparing their data with those reported in the literature. In addition, the extract was found to have potent hypoglycemic activity with IC_{50} of 5.62 ± 0.25 and 5.36 ± 0.24 μM, respectively, for α-glucosidase and α-amylase, while the most active fraction displayed inhibition effects with IC_{50} of 5.36 ± 0.24 and 5.20 ± 0.25 μM, respectively. Amongst the isolated compounds, kaempferol (**5**), and a mixture of β-sitosterol (**7**) and stigmasterol (**8**) were more active compared to acarbose (IC_{50} of 5.47 ± 0.27 μM) and quercetin (IC_{50} of 12.51 ± 0.13 μM) as the references. Moreover, kaempferol exhibited the strongest activity, which agrees with flavonoids biological properties. This observation was further explored by molecular docking studies, which suggested that kaempferol could bind favourably to the active sites of the target enzymes, supporting a potential competitive inhibition mechanism. This study contributed to enrich the chemistry of *Ceiba* plants with five known additional compounds (**1**, **2**, **3**, **6**, and **10**) and made *Ceiba pentandra* a promising source of antihypoglycemic compounds.
Keywords – *Ceiba pentandra*, Bombacaceae, Hypoglycemic, Bioactivity-guided, Molecular docking

Introduction

Diabetes mellitus is a condition in which the body's ability to produce or respond to the hormone insulin is impaired, leading to abnormal carbohydrate metabolism and elevated blood glucose levels.[1] Despite some available solutions, the number of deaths due to diabetes mellitus is still increasing. This could be the fact that some drugs have developed many side effects. In addition, the huge intake of insulin led to the problem of insulin resistance. A solution to the mentioned problems could be found in plant extracts or their natural products, as plants have been used as crude extracts to cure disease. *Ceiba pentandra* is a plant species belonging to the Bombacaceae family, which is widely distributed in tropical rainforests, including West and Central Africa. *Ceiba pentandra* is a tree with alternate leaves that grows up to 60 m high. In traditional folk medicine, the root, leaves, and bark extracts of *Ceiba pentandra* are used to treat hypotension, diabetes, dizziness, headaches, constipation, fever, and mental disorders.[2,3] Previous studies described the multimodal inhibition of α-Glucosidase and α-Amylase of the aqueous, methanol, and ethanol trunk bark extract of *Ceiba pentandra*.[4–7] In addition, the α-glucosidase activity of the ethanol root extract was also described.[8] From the above studies, the

*Author for correspondence
Samuel Magloire Bissim, Chemistry Laboratory, Faculty of Science, University of Bamenda BP: 039, Bambili, Cameroon
Tel: +237-696-435-792; E-mail: samuelbissim1@gmail.com, bissim.samuel@uniba.cm

Achille Nouga Bissoue, Process Engineering Laboratory, Department of Chemical Engineering, HTTTC, University of Douala, Douala, Cameroon
Tel: +237-699-977-923; E-mail: anbissoue@yahoo.fr

trunk and roots barks were screened to contain several secondary metabolites including saponins, flavonoids, tannins, triterpenes, and sterols,[4–8] while the LC-MS screening of the active whole plant extract revealed the presence of 22 different compounds, 8-(formyloxy)-8a-hydroxy-4a-methyldecahydro-2-naphtalene carboxylic acid, 2,4,6-trimethoxyphenol, 5,3′-dihydroxy-7,4′,5′-trimethoxyisoflavone, 17-hydroxylinoleicacid, and stigmasterol.[7] In the search for bioactive compounds from Cameroonian medicinal plants with antidiabetic properties,[9] *In Silico* and *in vitro* studies of the hypoglycemic chemical constituents of the methanolic root extract of *C. pentandra* were carried out by using a bioactivity-guided fractionation method. Based on these phytochemical and pharmacological studies, we discussed the structure-activity of the isolates and classified the plant species as a promising source of bioactive compounds in drug discovery to fight against diabetes.

Experimental

General experimental procedure – Column chromatography was performed using silica gel (70–230 mesh, E. Merck, Darmstadt, Germany). Thin-layer chromatography (TLC) was performed on Merck pre-coated silica gel 60 F_{254} aluminum sheets, and spots were detected using a diluted sulphuric acid spray reagent. A Hitachi UV-3200 spectrophotometer was used to record ultraviolet spectra in methanol. For ESI-MS and EI-MS, a Finnigan MAT 95 spectrometer (70 eV) was used with perfluorokerosene as a reference substance for HR-EI-MS. The ^{1}H- and ^{13}C-NMR spectra were recorded at 400/500 MHz and 100/125 MHz, respectively, on a Bruker AMX 500 NMR spectrometer, including COSY, HSQC, and HMBC experiments. Using tetramethylsilane (TMS) as the internal standard, chemical shifts are reported in δ (ppm), and coupling constants (J) were measured in Hz.

Plant material – The roots of *C. pentandra* were collected in Ebolowa, Cameroon, South region, more precisely at Metypkwale (3°54′0″ N and 11°54′0″ E), in February 2021. The plant was identified by Dr. TCHIENGUE of the National Herbarium of Cameroon, where a voucher specimen (43623/HNC) has been deposited.

Preparation of the crude extract – The air-dried and powdered roots of *C. pentandra* (2.00 kg) were macerated at room temperature for 48 hours with methanol (5 L). The obtained macerate was filtered and freeze-dried to give 100.50 g of total methanol crude extract.

Extraction and isolation of bioactive compounds – As the crude extract displayed interesting activity, a 75.00 g portion of the methanolic extract was subjected to open column chromatography eluted with *n*-Hexane, a mixture of *n*-Hexane/EtOAc, and EtOAc, increasing polarities. 100 fractions mL were collected and grouped based on TLC profiles into 8 major fractions (F_1–F_8). Fractions F_2 and F_8, which exhibited an interesting effect on the carbohydrate digestive enzymes, were selected for further steps. The other fractions were found to be inactive. An isocratic solvent system was used to purify F_2 [1500.80 mg, Hex-EtOAc (4:1, v/v)] in silica gel chromatography to give corosolic acid (**2**) (150.10 mg), α-amyrin (**3**) (100.15 mg), E-methylsuberenol (**6**) (40.17 mg), the mixture of β-sitosterol (**7**) and stigmasterol (**8**) (200.50 mg) and octadecanoic acid (**10**) (150.15 mg), while F_8 [1350.20 mg; Hex-EtOAc (3:2, v/v)] was purified on silica gel column chromatography with an isocratic solvent system of Hex-EtOAc (1:1, v/v) to give aridanin (**1**) (140.10 mg), quercetin (**4**) (50.35 mg), kaempferol (**5**) (20.05 mg), and β-sitosterol glucoside (**9**) (500.60 mg). All the isolated compounds from the active fractions (Fig. 1) were evaluated for their effect on carbohydrate enzymes. The structures of the isolated compounds were fully established by using spectroscopic (1D and 2D NMR, MS) experiments (supplementary data material), as well as by comparison with reported data.

Aridanin (**1**) – ^{1}H-NMR (400 MHz, DMSO-d_6): δ 0.65 (3H, s, H-24), 0.70 (3H, s, H-26), 0.84 (3H, s, H-29), 0.87 (3H, s, H-23), 0.88 (3H, s, H-25), 0.89 (3H, s, H-30), 1.12 (3H, s, H-27), 1.93 (3H, s, H_3CNAc), 3.0–4.2 (m, sugar protons), 4.41 (1H, d, J = 7.8 Hz, H-1′), 7.88 (1H, d, J = 9.2 Hz, NH); ^{13}C-NMR (100 MHz, DMSO-d_6): δ 15.2 (C-25), 16.1 (C-24), 16.8 (C-26), 17.8 (C-6), 22.7 (C-11), 22.9 (C-16), 23.2 (C-30), 25.2 (C-27), 25.6 (C-2), 28.6 (C-23), 29.1 (C-15), 30.5 (C-20), 32.2 (C-7), 32.5 (C-22), 32.8 (C-29), 33.2 (C-21), 36.2 (C-10), 38.1 (C-1), 38.2 (C-4), 40.7 (C-18), 41.2 (C-14), 45.5 (C-17), 47.6 (C-19), 47.0 (C-9), 54.9 (C-5), 55.8 (NCH_3), 61.3 (C-5′), 70.6 (C-3′), 74.1 (C-2′), 76.6 (C-4′), 88.2 (C-3), 103.5 (C-1′), 121.4 (C-12), 143.8 (C-13), 168.8 (NCO), 178.7 (C-28).

Corosolic acid (**2**) – ^{1}H-NMR (500 MHz, DMSO-d_6): δ 0.72 (3H, s, H-29), 0.74 (3H, s, H-30), 0.83 (3H, s, H-25), 0.91 (3H, s, H-24), 0.92 (3H, s, H-26), 0.92 (3H, s, H-27), 1.02 (3H, s, H-23), 4.23 (1H, d, J = 8.7 Hz, H-2β), 4.33 (1H, dd, J = 9.1, 11.5 Hz, H-3α), 5.18 (1H, t, J = 3.5 Hz, H-12), 3.43 (1H, t, J = 9.8 Hz, H-18), 2.75 (1H, t, J = 7.6 Hz, H-19), 2.10 (1H, t, J = 6.4 Hz, H-20); ^{13}C-NMR (125 MHz, DMSO-d_6): δ 178.1 (C-28), 138.1 (C-13), 124.5 (C-12), 82.2 (C-3), 67.2 (C-2), 54.7 (C-5), 52.3 (C-18), 47.1 (C-9), 46.8 (C-17), 46.7 (C-1), 41.6 (C-14), 39.1 (C-8), 38.9 (C-4), 38.4 (C-19), 38.4 (C-20), 37.6 (C-10),

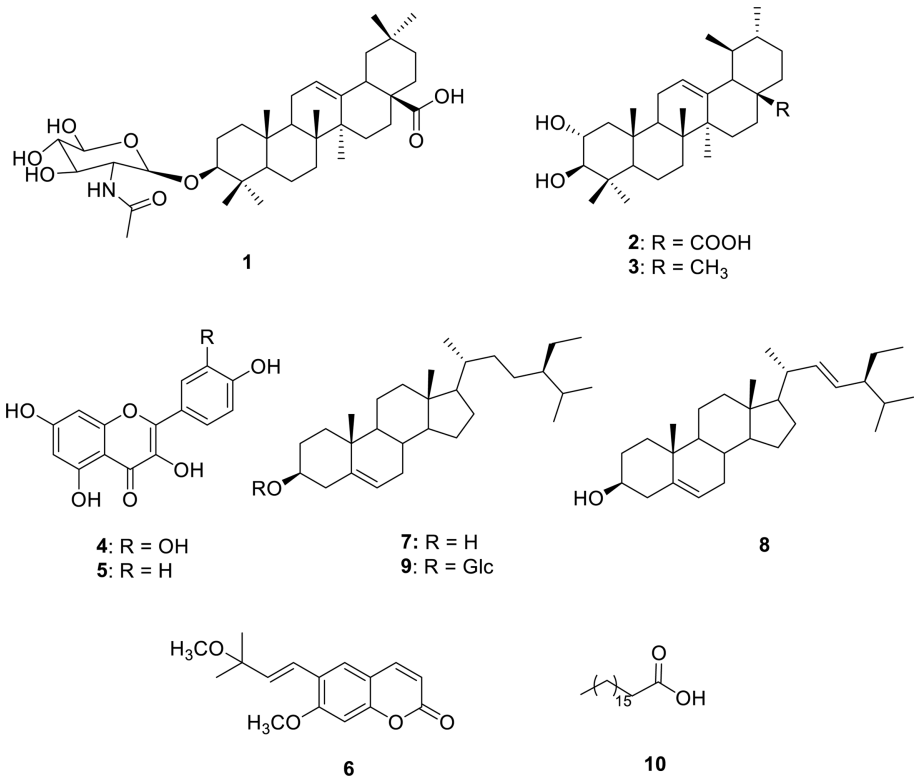

Fig. 1. Structure of isolated compounds **1–10** from the active fractions.

36.2 (C-22), 32.5 (C-7), 30.1 (C-21), 28.8 (C-23), 27.3 (C-15), 23.7 (C-16), 23.1 (C-27), 22.9 (C-11), 21.1 (C-29), 18.0 (C-6), 17.2 (C-24), 16.9 (C-26), 16.8 (C-30), 16.4 (C-25).

***α*-Amyrin** (**3**) – White amorphous powder; ^{1}H-NMR (CD_3OD, 500 MHz): δ 3.22 (1H, dd, J = 10.4, 5.1 Hz, H-3), 1.05–1.97 (21H, m, CH, CH_2), 5.10 (1H, t, J = 3.6 Hz, H-12), 0.98 (3H, s, H-23), 0.77 (3H, s, H-24), 0.92 (3H, s, H-25), 0.99 (3H, s, H-26), 1.03 (3H, s, H-27), 0.78 (6H, s, H-28 and H-29), 0.88 (3H, s, H-30); ^{13}C-NMR (125 MHz, DMSO-d_6): δ 139.5 (C-13), 124.3 (C-12), 79.6 (C-3), 59.1 (C-18), 55.1 (C-5), 47.8 (C-9), 42.1 (C-14), 41.5 (C-22), 40.7 (C-8), 39.6 (C-19), 39.5 (C-20), 38.7 (C-1), 36.6 (C-10), 33.8 (C-17), 32.2 (C-7), 31.2 (C-21), 28.4 (C-28), 27.2 (C-15), 26.6 (C-16), 23.4 (C-11), 23.2 (C-25, and C-27), 21.4 (C-30), 18.5 (C-6), 17.1 (C-29), 16.8 (C-24, and C-26), 15.5 (C-23).

Quercetin (**4**) – ^{1}H-NMR (CD_3OD, 500 MHz): δ 7.65 (1H, d, J = 2.1 Hz, H-2′), 7.51 (1H, dd, J = 8.4, 2.1 Hz, H-6′), 6.83 (1H, d, J = 8.4 Hz, H-5′), 6.40 (1H, d, J = 2.1 Hz, H-8), 6.20 (1H, d, J = 2.0 Hz, H-2).

Kaempferol (**5**) – ^{1}H-NMR (CD_3OD, 500 MHz): δ 6.20 (1H, d, J = 2.3 Hz, H-6), 6.41 (1H, d, J = 2.3 Hz, H-8), 8.01 (1H, d, J = 8.8 Hz, H-2′), 6.97 (1H, d, J = 8.5 Hz, H-3′), 6.97 (1H, d, J = 8.5 Hz, H-5′), 8.01 (1H, d, J = 8.5 Hz, H-6’); ^{13}C-NMR (125 MHz, CD_3OD): δ 98.2 (C-5), 93.5 (C-8), 129.5 (C-2′), 115.4 (C-5′), 129.5 (C-6′).

(*E*)-Methylsuberenol (**6**) – ^{1}H-NMR (CD_3OD, 500 MHz): δ 7.65 (1H, d, J = 9.3 Hz, H-4), 7.51 (1H, s, H-5), 6.80 (1H, s, H-8), 6.77 (1H, d, J = 16.6 Hz, H-12), 6.27 (1H, d, J = 9.3 Hz, H-3), 6.20 (1H, d, J = 16.6 Hz, H-11), 3.90 (3H, s, OCH_3), 3.23 (3H, s, OCH_3), 1.39 (6H, s, H-14,15).

Mixture of *β*-sitosterol (**7**) **and stigmasterol** (**8**) – White amorphous powder; ^{1}H-NMR ($CDCl_3$, 500 MHz): δ 1.15 (1H, m, H-1), 1.44 (11H, m, H-2, H-8, H-9, H-11, H-12, and H-14), 3.52 (1H, m, H-3), 1.98 (2H, m, H-4), 5.35 (1H, m, H-6), 1.85 (2H, m, H-7), 1.54 (4H, m, H-15, and H-16), 1.53 (1H, m, H-17), 0.68 (3H, s, H-18), 1.02 (3H, s, H-19), 2.27 (1H, m, H-20), 0.88 (3H, d, J = 6.3 Hz, H-21), 5.15 (3H, dd, J = 12.0, 8.0 Hz, H-22), 5.05 (3H, d, J = 12.0, 8.0 Hz, H-23), 2.23 (1H, m, H-24), 1.83 (1H, s, H-25), 0.86 (3H, d, J = 6.8 Hz, H-26), 0.82 (3H, d, J = 6.8 Hz, H-27), 1.26 (3H, m, H-28), 0.80 (3H, d, J = 6.3 Hz, H-29).

***β*-Sitosterol-3-*O*-*β*-D-glucopyranoside** (**9**) – White amorphous powder; ^{1}H-NMR (DMSO-d_6, 500 MHz): δ 1.24 (2H, m, H-1), 1.40 (2H, m, H-2), 3.46 (1H, m, H-3), 1.93 (2H, m, H-4), 5.33 (2H, m, H-6), 1.82 (2H, m, H-7), 1.51 (6H, m, H-8, H-9, H-11, H-12), 1.15 (1H, m, H-14),

1.81 (4H, m, H-15, and H-16), 1.24 (1H, m, H-17), 0.83 (3H, s, H-18), 0.95 (3H, s, H-19), 2.12 (1H, m, H-20), 0.91 (3H, d, J = 6.4 Hz, H-21), 1.50 (4H, m, H-24, H-26), 1.15 (2H, m, H-25), 1.63 (1H, m, H-27), 0.77 (3H, m, H-28), 0.99 (3H, d, J = 6.9 Hz, H-29), 4.23 (1H, d, J = 6.5 Hz, H-1′), 2.90 (1H, t, J = 7.0 Hz, H-2′), 3.12 (1H, d, J = 7.5 Hz, H-3′), 3.07 (1H, m, H-4′), 3.10 (1H, m, H-5′), 3.45 (1H, m, H-6′a), 3.68 (1H, m, H-6′b).

α-Amylase inhibition assay – The α-amylase inhibition assay was performed as described by Apostolidis and Lee,[10] with small modifications. Briefly, 50 μL of samples or acarbose was mixed with 50 μL of 0.02 M sodium phosphate buffer with α-amylase solution (13 U/mL) and incubated at 25°C for 10 min using a 1.5 mL tube. In addition, 50 μL of 1% soluble starch solution with 0.02 M sodium phosphate buffer was mixed into each well at regular intervals. The whole mixtures were then incubated at 25°C for 10 min, and 1 mL of dinitrosalicylic acid color reagent was added. The test tubes were then placed in boiling water for 10 min to stop the reaction and cooled to room temperature. The mixture was then diluted with 1 mL of distilled water, and the absorbance was read at 540 nm using a 96-well microplate reader. The inhibition of α-amylase was expressed as a percentage of inhibition and calculated as follows:

$$\% \text{ Inhibition} = \frac{\text{Absorbance of control} - \text{Absorbance of sample}}{\text{Absorbance of control}} \times 100$$

α-Glucosidase inhibition assay – The α-glucosidase inhibition assay was performed as described by Honda and Hara,[11] with small modifications. To determine the activity of α-glucosidase, 10 μL of the sample was mixed with 140 μL of buffer solution, and 100 μL of enzyme was added; then the above mixture was submitted for incubation at 37°C for 10 min; subsequently, 200 μL of substrate was added, and the mixture was incubated once again at 37°C for 20 min. Later on, 1000 μL of sodium carbonate was added, and the absorbance was measured at 405 nm. The inhibition of α-glucosidase was expressed as a percentage of inhibition and calculated as follows:

$$\% \text{ Inhibition} = \frac{\text{Absorbance of control} - \text{Absorbance of sample}}{\text{Absorbance of control}} \times 100$$

β-Galactosidase inhibition assay – 10 μL of sample was mixed with 140 μL of buffer solution 7.6, and 100 μL of enzyme was added. The above mixture was submitted for incubation at 37°C for 10 min; then 200 μL of substrate was added, and the resulting mixture was incubated once at 37°C for 20 min. After incubation, 1000 μL of 0.1 M sodium carbonate was added, and the absorbance was measured at 410 nm.[10] The percentage of inhibition of the β-galactosidase was expressed according to the above formula for α-galactosidase.

Ligand preparation – The 3D ligand structures were retrieved from PubChem (https://pubchem.ncbi.nlm.nih.gov) in SDF format and prepared using Schrödinger's LigPrep tool (Release 2017-2), generating tautomeric forms and minimizing energy with the OPLS3 force field.[12]

Protein preparation – Enzyme structures: alpha-amylase (PDB: 3BC9), alpha-glucosidase (PDB: 3W37) and beta-galactosidase (PDB: 6TTE), were downloaded from the Protein Data Bank and prepared via Schrödinger's Protein Preparation Wizard: adding hydrogens, removing waters, assigning partial charges (OPLS-2003 force field), protonating residues and minimizing energy (0.3 Å RMSD limit). Receptor grids (20 Å^3) were generated centered on native ligands, with van der Waals scaling of 1.00 and partial charge cutoff of 0.25.

Molecular docking – The ligands were precisely positioned within the active site of each enzyme using standard precision (SP) mode in Glide without any constraints, and specific parameters included a van der Waals radius scaling factor of 0.80 and a partial charge cut-off of 0.15. To estimate binding affinity and rank ligands, GlideScore, implemented in the Glide software (Maestro, version 11.8 (2018) Schrödinger, LCC, New York), was employed.

Results and Discussion

The methanolic crude extract was prepared from the roots of *C. pentandra*. This extract displayed significantly higher α-amylase and α-glucosidase inhibitory activities than acarbose, which was used as the reference (IC_{50} of 5.27 ± 0.14 μM, IC_{50} of 5.47 ± 0.27 μM), while it was less active than quercetin (IC_{50} of 12.51 ± 0.13 μM), used as a reference against β-galactosidase inhibitory activity (Table 1). The results obtained are consistent with those reported by Nguelefack and collaborators[4] on the methanolic trunk bark extract. A bioguided fractionation was performed with the perspective of the identification of phytocompounds that can be responsible for the activity. From the fractionation, fractions F_2 and F_8 exhibited significant activities and were subjected to further analysis.

Table 1. The hypoglycemic properties of extract, fractions, and isolated compounds **1**–**10**

Samples	IC_{50} ± SEM (μM)		
	β-galactosidase	*α*-glucosidase	*α*-amylase
Methanolic extract	14.33 ± 0.23^{ab}	5.62 ± 0.25^{cb}	5.36 ± 0.24^{aa}
F_2	/	5.36 ± 0.24^{cb}	8.48 ± 0.22^{aa}
F_8	/	5.78 ± 0.23^{cb}	5.20 ± 0.25^{aa}
1	17.22 ± 0.16^{g}	06.25 ± 0.01^{e}	12.63 ± 0.05^{h}
2	06.47 ± 0.43^{e}	11.90 ± 0.05^{g}	08.09 ± 0.40^{g}
3	ND	ND	ND
4	ND	ND	ND
5	05.58 ± 0.30^{d}	03.33 ± 0.22^{b}	5.03 ± 0.18^{a}
6	ND	ND	ND
7	ND	ND	ND
7 and **8**	5.03 ± 0.11^{abc}	3.13 ± 0.20^{ab}	5.35 ± 0.01^{c}
9	ND	ND	ND
10	ND	ND	ND
Acarbose	-	5.47 ± 0.27^{ca}	5.22 ± 0.14^{aa}
Quercetin	12.51 ± 0.13^{aa}	-	-

Fractions F_2 and F_8 were fully chromatographed, from which ten known compounds were isolated (Fig. 1). The isolates were fully characterized by using 1D (^{1}H, ^{13}C), 2D NMR spectroscopic and spectrometric techniques, then by comparison with the reported data in literature (Supplementary data material is given). The successive chromatography of F_2 and F_8 allowed us to identify the following isolates: three terpenoids [aridanin (**1**),[13] corosolic acid (**2**), and *α*-amyrin (**3**)],[14] two flavonoids namely [quercetin (**4**) and Kaempferol (**5**)],[15] one coumarin [(*E*)-methylsuberenol (**6**)],[16] one acid [octadecanoic acid (**10**)][7] and three common steroids, [the mixture of *β*-sitosterol (**7**) and stigmasterol (**8**), and *β*-sitosterol glucoside (**9**)].[17]

Extracts, fractions, and isolated compounds were all subjected to *α*-amylase inhibitory potency. Table 1 contains the results obtained. For all tested compounds, aridanin (**1**), kaempferol (**5**), corosolic acid (**2**), a mixture of stigmasterol (**8**) and *β*-sitosterol (**7**), displayed a significant *α*-amylase inhibitory activity in comparison with acarbose used as the reference (IC_{50} of 5.22 ± 0.14 μM). The most active compound for *α*-amylase inhibition was kaempferol (**5**) (IC_{50} of 5.03 ± 0.18 μM), which is more active than acarbose.

For further assessment of hypoglycemic properties, the *α*-glucosidase inhibitory activity was performed. The study revealed good potential anti-*α*-glucosidase activity components like kaempferol (**5**), stigmasterol (**8**), and *β*-sitosterol (**7**) mixture in comparison with acarbose (IC_{50} of 5.47 ± 0.27 μM) used as reference. Amongst the latter, the most active was the mixture of *β*-sitosterol (**7**) and stigmasterol (**8**) (IC_{50} of 3.13 ± 0.20 μM). This result is consistent with that of Lolok and collaborators.[13]

Amongst all the tested compounds, aridinin (**1**), corosolic acid (**2**), kaempferol (**5**), mixture of *β*-sitosterol (**7**) and stigmasterol (**8**) displayed significant *β*-galactosidase inhibitory activity. The mixture of stigmasterol (**8**) and *β*-sitosterol (**7**) is the most active in this series of components, with an IC_{50} of 5.03 ± 0.11 μM in comparison with quercetin (IC_{50} of 12.51 ± 0.13 μM) used as reference. In addition, stigmasterol was proven to act through different mechanisms of action, including the reduction of intestinal glucose absorption, insulin receptor stimulation, and the enhancement of GLUT4 receptors.[18–20] Triterpene corosolic acid previously reported to exhibit hypoglycemic activity with significant activity through inhibition of *α*-glucosidase enzyme,[17] whilst aridanin is revealed here to act against *α*-amylase and *β*-galactosidase, and reported for the first time to our best knowledge.

The bioactivity-guided and phytochemical investigation of the root methanolic extract of *C. pentandra* led to the structural elucidation of ten known compounds as follows: three triterpenes **1**–**3**, two flavonoids **4** and **5**, one coumarin **6**, three sterols **7**–**9**, and one fatty acid **10**. To our best knowledge, compounds **1**, **2**, **3**, **6**, and **10** were reported here for the first time from the *Ceiba* genus; the rest were isolated from other species of the *Ceiba* genus, and *C. pentandra*.[3,21] Moreover, quercetin (**4**) was previously reported from the bark of *C. speciosa*[22] and the fruit of *C. aesculifolia*,[23] while kaempferol was isolated from the bark of *C. speciose*,[22] and sterols were isolated from *C. crispiflora*.[24] In this study, the chemotaxonomic significance of the species brings here a new source of triterpenes skeleton of the oleanane series, like corosolic acid (**2**), *α*-amyrin (**3**), and aridanin (**1**).

The docking protocol was first validated for each target enzyme by redocking the native co-crystallized ligand into the prepared binding site. The native and redocked ligand conformations were then superimposed, as shown in Fig. 2, and the root-mean-square deviation (RMSD) between the docked pose and the original crystallographic conformation was calculated. For α-amylase (PDB ID: 3BC9, native ligand: *α*-acarbose), an RMSD value of 1.44 Å was obtained. For *α*-glucosidase (PDB ID: 3W37, native ligand: alpha-acarbose), the RMSD was 1.53 Å. For *β*-galactosidase (PDB ID: 6TTE, native ligand: *β*-D-galactopyranoside), the RMSD was 0.26 Å. As RMSD

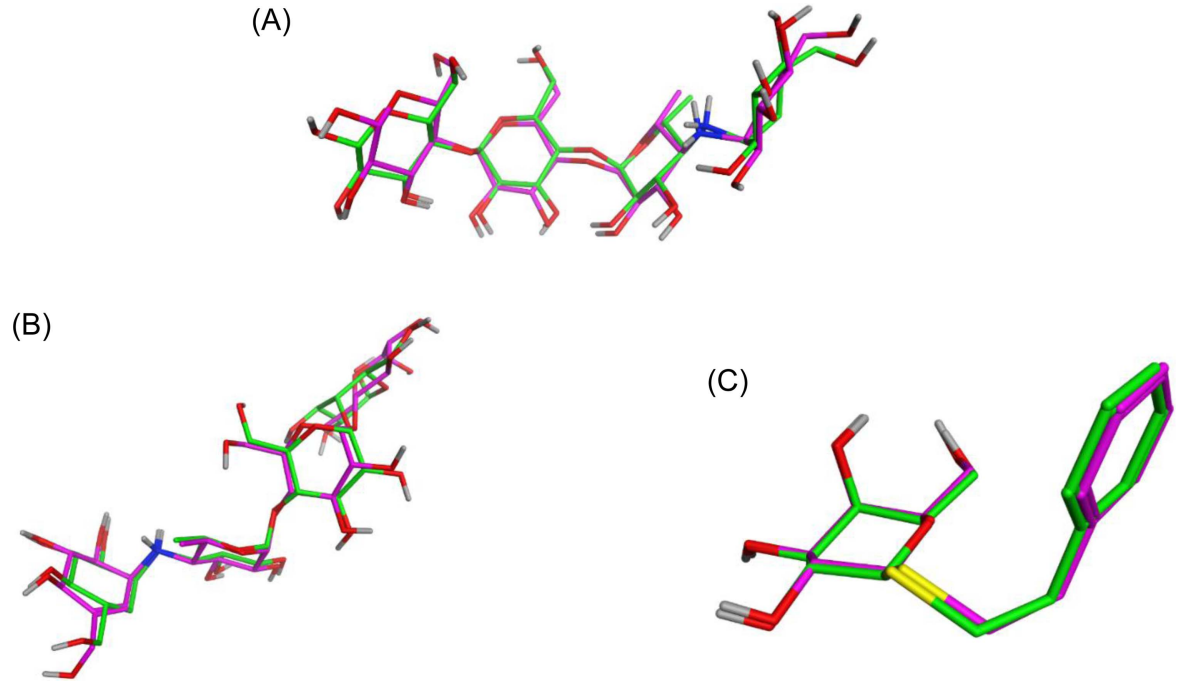

Fig. 2. Superposition of the native co-crystallized ligands (shown in green) and their corresponding redocked poses (shown in pink) within the active sites of: A) α-amylase (PDB ID: 3BC9), B) α-glucosidase (PDB ID: 3W37), and C) β-galactosidase (PDB ID: 6TTE).

values below 2.0 Å are generally considered acceptable, these results confirm that the applied docking parameters are capable of reliably reproducing the experimental binding modes for each enzyme system.

Molecular docking studies were conducted to gain insights into the molecular mechanisms underlying the activity of the compounds against key diabetes-related enzymatic targets, including alpha-amylase, alpha-glucosidase, and beta-galactosidase.

Docking scores of the compounds that exhibited inhibitory activity against *α*-amylase are summarized in Table 2. The docking scores provided qualitative insights into potential binding affinities. Kaempferol, which exhibited slightly higher inhibitory activity (IC_{50} = 5.03 μM) than acarbose (IC_{50} = 5.22 μM), showed a comparable docking score (−6.410 kcal/mol vs. −6.445 kcal/mol for acarbose). It is important to note that a difference of < 1 kcal/mol is within the typical margin of error for molecular docking and should not be overinterpreted. Nevertheless, the similar scores are consistent with their comparable *in vitro* potency. This correlation between biological activity and binding affinity to alpha-amylase was also observed for aridanin, which showed poor penetration into the enzyme's active site (docking score = −2.457 kcal/mol) and reduced inhibitory activity (IC_{50} = 12.63 μM). The stigmasterol/beta-sitosterol mixture exhibited inhibitory activity (IC_{50} = 5.35 μM) almost like that of the reference ligand, although the individual docking scores for both compounds (−4.90 kcal/mol) were less favourable than that of acarbose. This suggests that the observed inhibitory effect may be more than additive, possibly involving complementary or cooperative interactions at the enzymatic level. These results are consistent with those observed by Payghami and collaborators[25] regarding the synergistic effect of sterols on the enzymatic activity of *α*-amylase.

Table 2. Docking score values indicating the binding affinities of tested compounds toward *α*-amylase, *α*-glucosidase, and *β*-galactosidase

Compounds	Docking Score (Kcal/mol)		
	α-amylase	*α*-glucosidase	*β*-galactosidase
Acarbose	−6.445	−6.525	-
Kaempferol	−6.410	−6.691	−5.22
Stigmasterol	−4.910	−4.183	−3.00
β-sitosterol	−4.920	−4.026	−3.56
Aridanin	−4.457	−3.560	−2.01
Corosolic acid	−4.334	−2.050	−6.10
Quercetin	-	-	−6.14

The analysis of molecular interactions, as illustrated in the 2D interaction diagrams presented in Fig. 3A and 3B,

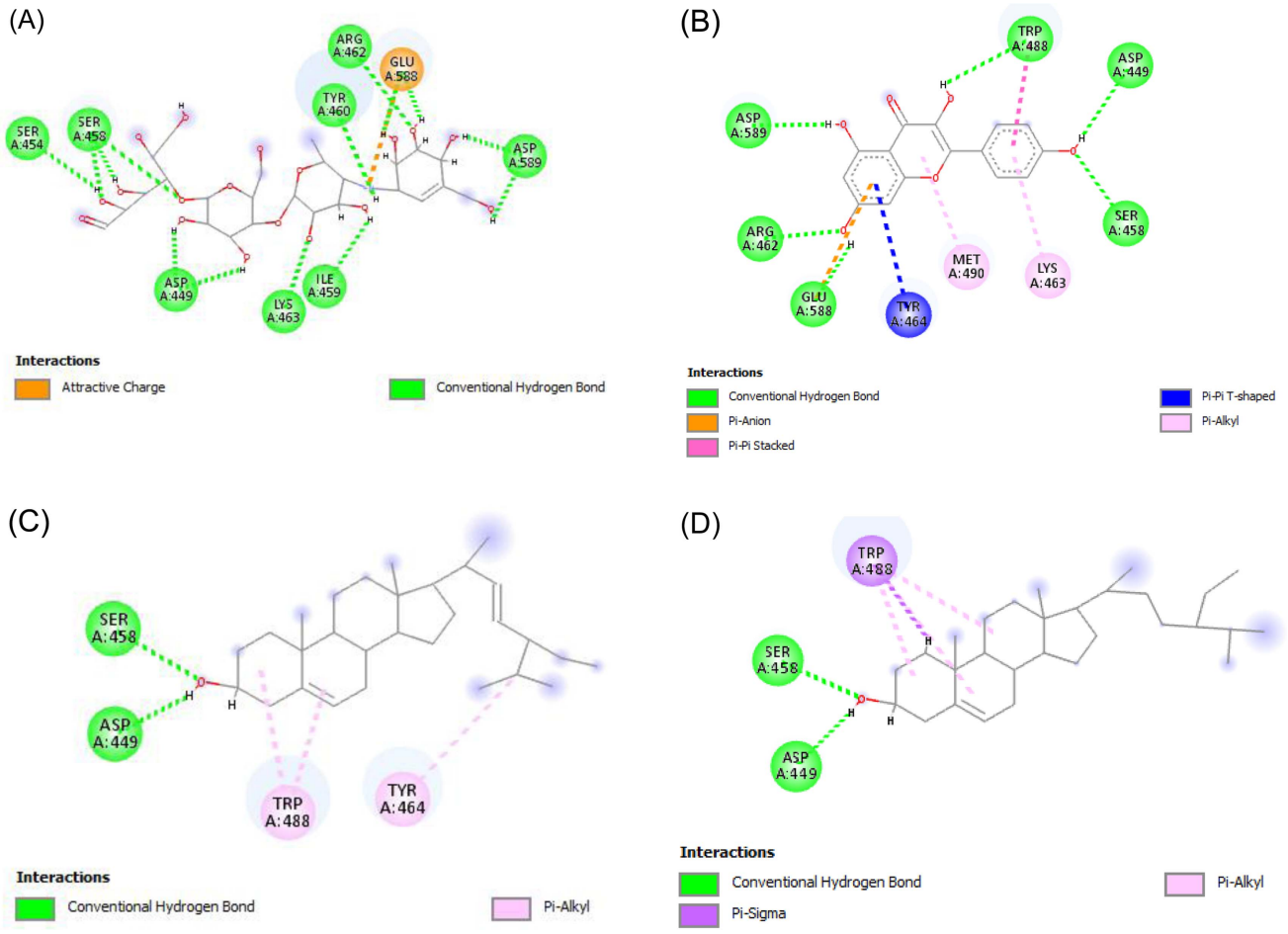

Fig. 3. 2D interaction diagrams of the 3BC9 protein in complex with (A) reference ligand, (B) Kaempferol, (C) stigmasterol, and (D) *β*-sitosterol.

reveals that both kaempferol and the reference ligand establish a dense and diverse network of interactions with the residues within the active site, which likely accounts for their high binding affinities. The reference ligand (Fig. 3A) forms up to ten hydrogen bonds with active site residues, including Ser458 (three hydrogen bonds), Asp499 (two), Glu588 (two), and single interactions with Lys463, Ile459, Asp589, Ser454, Arg462, and Tyr460. Additionally, favourable electrostatic (attractive charge) interaction with Glu588 likely contributes significantly to the stability of the ligand-enzyme complex. Kaempferol (Fig. 3B) also forms multiple hydrogen bonds with key residues such as Asp589, Arg462, Glu588, Ser458, Asp449, and Trp448. This hydrogen bonding network is further completed by a range of hydrophobic and aromatic interactions, including Pi-anion (Glu588), Pi-Pi stacking (Trp488), Pi-Pi T-shaped (Tyr464), and Pi-alkyl interactions (Lys463 and Met490), underscoring the compound's strong and diverse binding profile. In contrast, stigmasterol and *β*-sitosterol exhibit a more limited set of specific interactions. Stigmasterol (Fig. 3C) forms two hydrogen bonds with Ser458 and Asp449, along with Pi-alkyl interactions involving Trp448 and Tyr464. Similarly, *β*-sitosterol (Fig. 3D) forms two hydrogen bonds with the same residues as stigmasterol and engages in a Pi-alkyl and a Pi-sigma interaction with Trp488. The reduced interaction coverage, limited hydrogen bonding, and lack of ionic interactions likely explain the weaker binding affinities (reflected by higher docking scores) of these two compounds compared to the reference ligand and kaempferol.

The docking results of the compounds exhibiting activity against *α*-glucosidase are summarized in Table 2. Kaempferol displayed the highest predicted binding affinity toward this enzyme, with a docking score of −6.691 kcal/mol, which was slightly more favorable than that of the reference ligand (−6.525 kcal/mol). For kaempferol, this computational prediction is in line with the *in vitro* data (Table 1), which showed a lower IC_{50}

value compared to the reference compound. This consistency supports the notion that kaempferol could act as a competitive inhibitor of alpha-glucosidase, as previously suggested by Uyanir and collaborators.[26] On the other hand, the docking scores for aridanin (−3.560 kcal/mol) and corosolic acid (−2.050 Kcal/mol) were less favorable, which is consistent with their relatively weaker inhibitory activities observed *in vitro* (Table 1). Stigmasterol and *β*-sitosterol showed lower binding affinities, with docking scores of −4.118 and −4.026 kcal/mol, respectively. However, the combination of these two phytosterols exhibited significantly enhanced inhibitory activity (IC_{50} = 3.13 μM) compared to the reference ligand (IC_{50} = 5.47 μM). This suggests a possible synergistic interaction between the two compounds, which may account for the improved biological efficacy despite their individually modest docking scores.

To better understand the mechanism of action and the nature of the interactions formed between the various ligands and *α*-glucosidase, 2D interaction diagrams were constructed for the reference ligand, kaempferol, stigmasterol, and *β*-sitosterol. The 2D diagram of the reference ligand (Fig. 4A) reveals the formation of multiple hydrogen bonds with key catalytic residues: Asp630 (two bonds), Asp232 (two bonds), Asp357 (two bonds), Asp568, and Arg552. Additionally, attractive charge interactions were observed with Asp568 (two interactions), Asp469 (two), and Asp232. Kaempferol (Fig. 4B) forms hydrogen bonds with residues Asp469, Asp357, Arg552, Asp558, and Asp630, and a Pi-cation interaction with Asp568 and a Pi-alkyl interaction with Ala628 further stabilize the binding. The interaction network is completed by three Pi-Pi T-shaped interactions involving Phe601 (two interactions) and Trp329. Stigmasterol (Fig. 4C) and *β*-sitosterol (Fig. 4D) exhibited similar interaction profiles. Both compounds formed a hydrogen bond with Glu603 and established several Pi-alkyl interactions with hydrophobic residues, including Phe601 (two interactions), Trp329 (two), Phe236, and Trp432.

The docking analysis provided insights into the potential molecular interactions that may underline the observed inhibitory activity against *α*-glucosidase. For

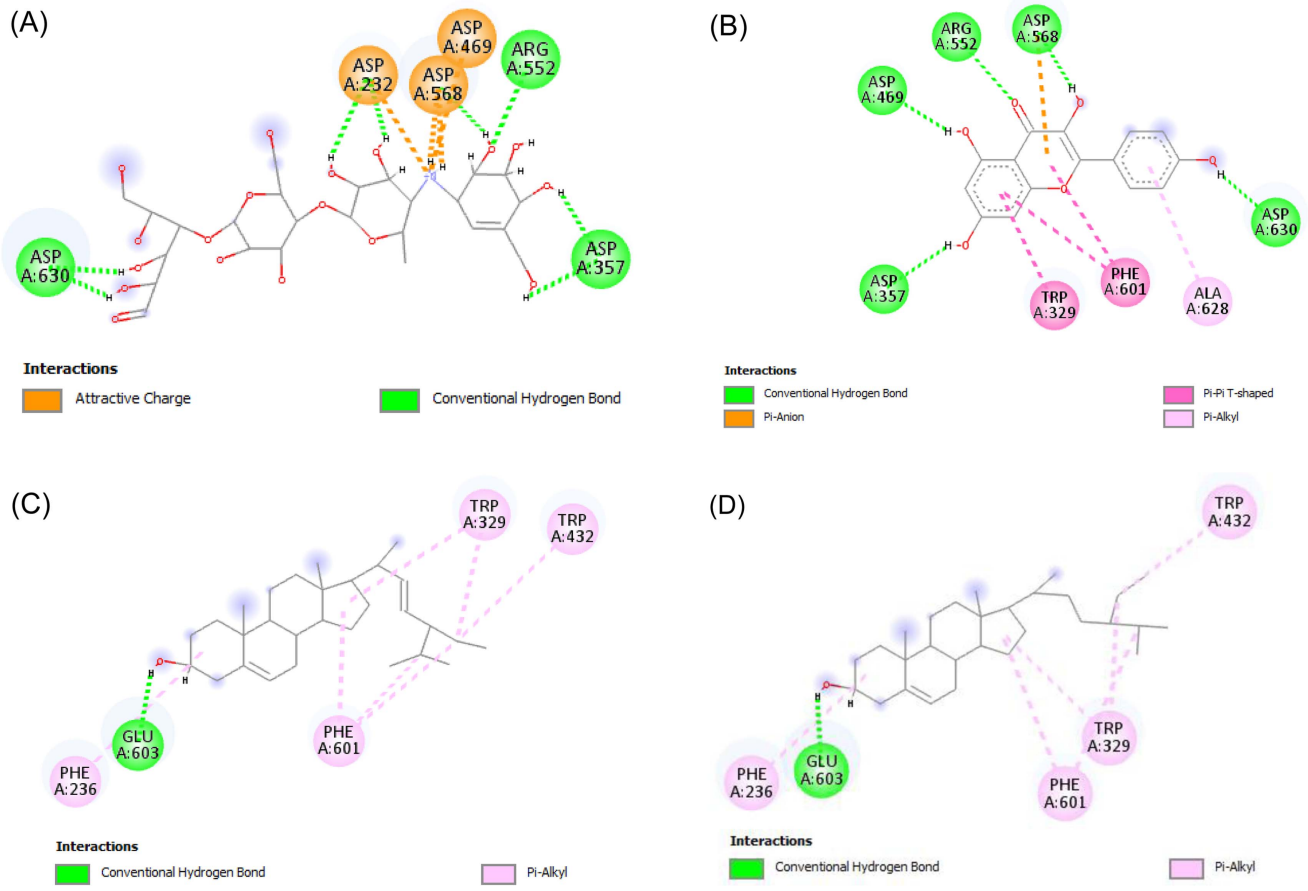

Fig. 4. 2D interaction diagrams of the 3W37 protein in complex with (A) reference ligand, (B) Kaempferol, (C) stigmasterol, and (D) *β* -sitosterol.

instance, both kaempferol and the reference ligand formed multiple polar interactions with key catalytic aspartate residues, which could explain their relatively higher binding affinities and biological activities, consistent with a potential competitive inhibition mechanism.

The docking scores of the compounds exhibiting activity against beta-galactosidase are summarized in Table 2. Kaempferol and corosolic acid, which showed stronger biological activity against this enzyme compared to the reference ligand (quercetin), present docking scores comparable to those of quercetin. The binding affinities reported for quercetin, corosolic acid, and kaempferol are −6.14, −6.10, and −5.22 kcal/mol, respectively. A good correlation between biological activity and binding affinity was observed for aridanin, which exhibited both a higher IC_{50} value and docking score compared to the other compounds, indicating lower inhibitory potential. Interestingly, despite displaying the highest predicted binding affinity, quercetin showed only moderate biological activity. This discrepancy may be attributed to possible destabilization of the *β*-galactosidase-quercetin complex under physiological conditions.

To gain insights into the origin of the observed binding affinities, 2D interaction diagrams of the various ligands within the active site of beta-galactosidase were constructed. These diagrams illustrate the key molecular interactions stabilizing each ligand-enzyme complex. The 2D interaction diagram of the reference ligand quercetin (Fig. 5A) shows the formation of three hydrogen bonds with Lys517, Asn102, and Asp201. Additionally, quercetin engages in three Pi-Pi T-shaped interactions with Tyr503 (two interactions) and Trp568, along with Pi-Pi stacked, Pi-sulfur, Pi-anion, and Pi-cation interactions involving Trp999 (two interactions), Met502 (two interactions), Glu461, and the catalytic Mg^{2+} ion (MG3001), respectively. Kaempferol (Fig. 5B) is stabilized by two hydrogen bonds with Asp201 and Asn102 (two interactions), and by a Pi-alkyl interaction with Met502. It also forms Pi-Pi T-shaped, Pi-Pi stacked, Pi-sulfur, Pi-anion, and Pi-cation interactions involving the same residues as quercetin. However, unlike quercetin, kaempferol lacks the hydrogen bond with the key residue Lys517 but features a Pi-alkyl interaction with Met502. This slight difference in the interaction network may explain its relatively higher docking score (i.e., lower predicted affinity) compared to quercetin. The moderate biological activity of quercetin (as reported in Table 1) may be attributed to the instability of the *β*-galactosidase-quercetin complex under physiological conditions. This phenomenon was also observed in the study by Kitchen and collaborators[27] under physiological conditions. Corosolic acid (Fig. 5C) is stabilized by two hydrogen bonds with Asp201 and Trp999, a metal-acceptor interaction with MG3001, an attractive charge interaction with Lys517, and multiple Pi-alkyl interactions with His418, Tyr503, His540, and Trp999. The strong binding affinity (low docking score) of corosolic acid can be attributed to its diverse interaction profile and the formation of critical interactions with key residues such as Asp201, Lys517, and MG3001. The interaction diagrams of the sterols (Fig. 5D and 5E) display less diverse interaction profiles compared to the other ligands, which may explain their lower binding affinities toward *β*-galactosidase. Stigmasterol (Fig. 5D) forms a single hydrogen bond with Asp598, two Pi–sigma interactions with Trp999 and Phe601, and three Pi–alkyl interactions with His418, Trp999, and Phe601. In contrast, beta-sitosterol (Fig. 5E) forms two hydrogen bonds with Lys517 and Glu487, as well as several Pi-alkyl interactions with Phe601, His418, and Trp999. The relatively higher affinity of *β*-sitosterol compared to stigmasterol is likely due to the presence of a hydrogen bond with the key catalytic residue Lys517.

It is important to acknowledge the limitations of the molecular docking approach employed in this study. The docking scores represent static, simplified estimates of binding affinity. The inconsistent correlation between docking scores and IC_{50} values for some compounds (e.g., quercetin vs. kaempferol on *β*-galactosidase) underscores the complexity of biological inhibition, which involves factors beyond static binding (e.g., solvation effects, entropy, protein dynamics). Therefore, the docking results are presented as supportive computational evidence that aids in the interpretation of the experimental findings and suggests potential binding modes, rather than as conclusive proof of mechanism.

In conclusion, this study describes the bioactivity-guided phytochemical investigation of the methanolic root extract of *C. pentandra*. From the active fractions, the study led to the isolation and structural identification of ten known compounds (**1**–**10**) classified under various classes of secondary metabolites as follows: three triterpenes **1**–**3**, two flavonoids **4** and **5**, one coumarin **6**, three sterols **7**–**9**, and one fatty acid **10**. To the best of our knowledge, amongst the isolates, compounds **1**, **2**, **3**, **6**, and **10** were reported here for the first time from the *Ceiba* genus. The crude extract, fractions, and isolated compounds were tested for their hypoglycemic activity against *α*-glucosidase, *α*-amylase, and *β*-galactosidase inhibitory activity using acarbose as a reference for *α*-amylase and *α*-glucosidase, and quercetin for *β*-galacto-

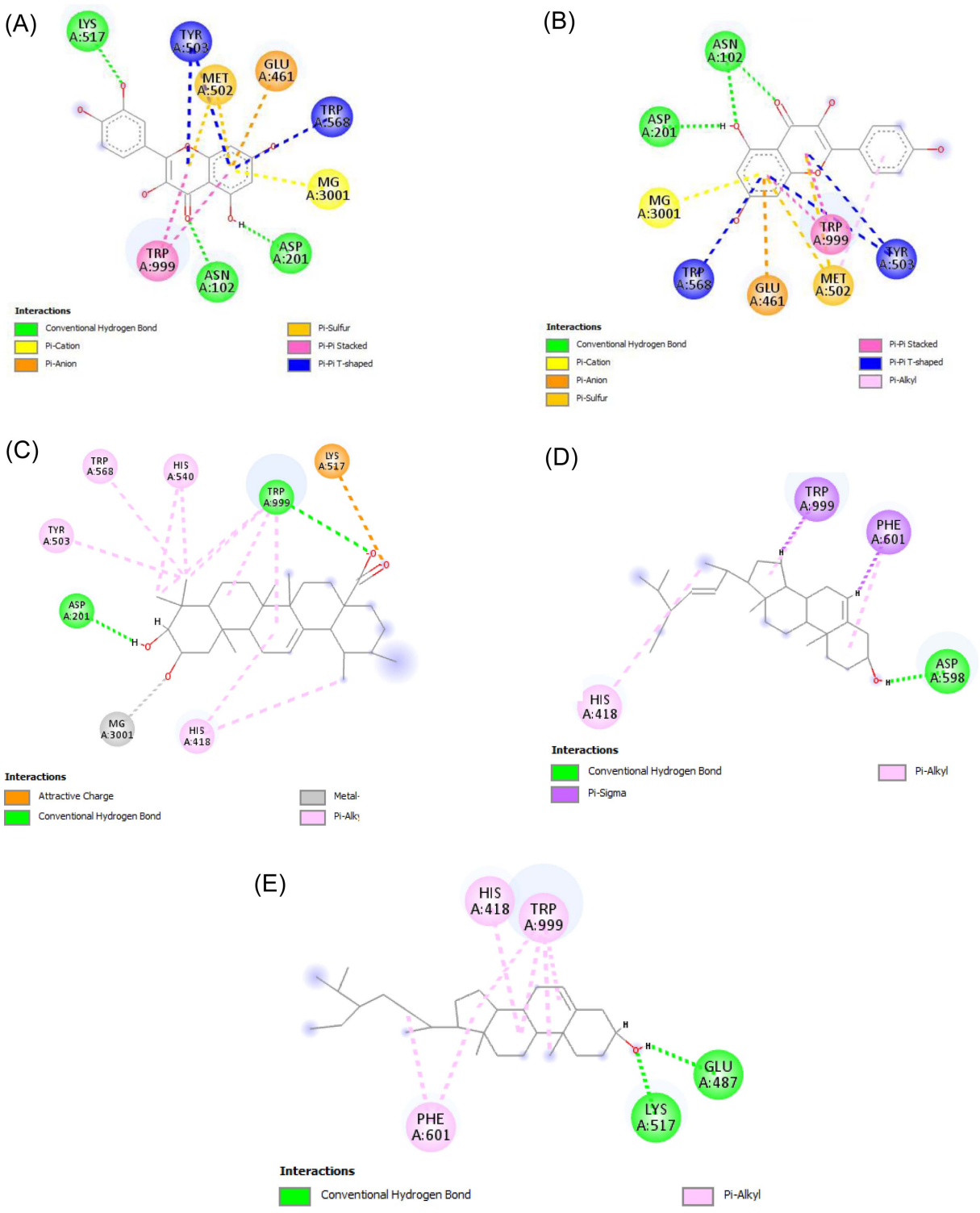

Fig. 5. 2D interaction diagrams of the 6TTE protein in complex with (A) reference ligand, (B) Kaempferol, (C) corosolic acid, (D) stigmasterol, and (E) *β*-sitosterol.

sidase. The study showed that the most active compounds were kaempferol (**5**), a mixture of *β*-sitosterol (**7**) and Stigmasterol (**8**), which agrees with reported data of flavonoids and sterols. Molecular docking analyses provided supportive, qualitative insights into the potential binding modes of the active compounds. The observed

interaction profiles, such as the multiple hydrogen bonds formed by kaempferol with catalytic residues, were consistent with a plausible competitive inhibition mechanism and complemented the *in vitro* activity data. The significantly higher activity of the stigmasterol and *β*-sitosterol mixture compared to the individual components suggests that their combined effect may be more than additive, possibly involving complementary or cooperative interactions at the enzymatic level. The study highlights the utility of combining *in vitro* assays and *in silico* approaches to form a more coherent picture of potential bioactivity, while acknowledging the inherent limitations of static docking simulations. It is also showed that the chemical study of *Ceiba pentandra* enrich the number of active secondary metabolites isolated from this genus with triterpenes skeleton of the oleanane series, corosolic acid (**2**), *α*-amyrin (**3**), and aridanin (**1**). Further research on the toxicity and *in vivo* bioassay may be necessary to support the effectiveness of the enzymatic properties of those compounds.

Acknowledgements

The author is grateful to Dr. Barthelemy TCHIENGUE of the National Herbarium of Cameroon for harvesting and identifying the plant material.

Conflicts of Interest

The authors have no relevant financial interests to disclose.

References

(1) Sacks, D.; Arnold, M.; Bakris, G. L.; Bruns, D. E.; Horvath, A. R.; Lernmark, A.; Metzger, B. E.; Nathan, D. M.; Kirkman, M. *Diabetes care* **2023**, *46*, 10, e151–e199.

(2) Ladeji, O.; Omekarah, I.; Solomon, M. *J. Ethnopharmacol.* **2003**, *84*, 139–142.

(3) Ngounou, F.; Meli, A. L.; Lontsi, D.; Sondengam, B. L.; Atta-Ur-Rahman; Choudhary, M. I.; Malik, S.; Akhtar. F. *Phytochemistry* **2000**, *54*, 107–110.

(4) Nguelefack, T. B.; Fofie, C. K.; Nguelefack-Mbuyo, E. P.; Kaptue Wuyt, A. *Biomed. Res. Int.* **2020**, *2020*, 3063674.

(5) Syihabudin, V.; Sari, B. L.; Utami, N. F.; Aprialini, N. A.; *Indonesian J. Pharm.* **2018**, *29*, 206–213.

(6) Mun'im, A.; Katrin, K.; Azizahwati, A.; Andriani, A.; Mahmudah, K. F.; Mashita, M. *Int. J. Med. Aromat. Plants* **2013**, *3*, 144–150.

(7) Fodem, C.; Nguelefack-Mbuyo, E. P.; Ndjenda, M. K.; Kamanyi, A.; Nguelefack, T. B. *Biomed. Res. Int.* **2021**, *2021*, 4730341.

(8) Bothon, F. T. D.; Debiton, E.; Yedomonhan, H.; Avlessi, F.; Teulade, J.-C.; Sohounhloue, D. C. K. *Res. J. Chem. Sci.* **2012**, *2*, 31–36.

(9) Ngolong, R. L. B. N.; Tabekoueng, G. B.; Happi, G. M.; Wansi, J. D. *Nat. Resour. Human Health* **2024**, *4*, 189–193.

(10) Apostolidis, E.; Lee, C. M. *J. Food Sci.* **2010**, *75*, H97–H102.

(11) Honda, M.; Hara, Y. *Biosci. Biotechnol. Biochem.* **1993**, *57*, 123–124.

(12) Harder, E.; Damm, W.; Maple, J.; Wu, C.; Reboul, M.; Xiang, J. Y.; Wang, L.; Lupyan, D.; Dahlgren, M. K.; Knight, J. L.; Kaus, J. W.; Cerutti, D. S.; Krilov, G.; Jorgensen, W. L.; Abel, R.; Friesner, R. A. *J. Chem. Theory. Comput.* **2016,** *12*, 281–296.

(13) Lolok, N.; Sumiwi, S. A.; Sahidin, I.; Levita, *J. World. Acad. Sci. J.* **2023**, *5*, 25.

(14) Wahyuni, Y. *Media Keperawatan Indonesia* **2021**, *4*, 234–246.

(15) Wang, J.; Huang, M.; Yang, J.; Ma, X.; Zheng, S.; Deng, S.; Huang, Y.; Yang, X.; Zhao, P. *Food Nutr. Res.* **2017**, *61*, 1339556.

(16) Indradevi, S.; Ilavenil, S.; Kaleeswaran, B.; Srigopalram, S.; Ravikumar, S. *J. King. Saud. Univ. Sci.* **2011**, *24*, 2, 171–177.

(17) Hou, W.; Li, Y.; Zhang, Q.; Wei, X.; Peng, A.; Chen, L.; Wei, Y. *Phytother. Res.* **2009**, *23*, 614–618.

(18) Mbaveng, A. T.; Chi, G. F.; Bonsou, I. N.; Abdelfatah, S.; Tamfu, A. N.; Yeboah, E. M. O.; Kuete, V.; Efferth, T. *Phytomedicine* **2020**, *76*, 153261.

(19) Batubara, I.; Suparto, I. H.; Wulandari, N. S. *Earth Environ. Sci.* **2017**, *58*, 012060.

(20) Ju Ichi, M.; Inoue, M.; Ikegami, *Heterocycles* **1988**, *27*, 1451–1454.

(21) Bravo, J. A.; Lavaud, C.; Bourdy, G.; Deharo, E.; Giménez, A.; Sauvain, M. *Bol. J. Chem.* **2002**, *1*, 18–24.

(22) Malheiros, C. K. C.; Silva, J. S. B.; Hofmann, T. C.; Messina, T. M.; Manfredini, V.; Piccoli, J. da C. E.; Faoro, D.; Oliveira, L. F. S.; Machado, M. M.; Farias, F. M. *Braz. J. Pharm. Sci.* **2017**, *53*, e16098.

(23) Franco, B. M.; Jiménez-Estrada, M.; Hernández - Hernández, A. B.; Hernández, L. B.; Rosas- López, R.; Durán, A.; Rodríguez-Monroy, M. A.; Canales-Martínez, M. *Afr. J. Tradit. Complement Altern. Med.* **2016**, *13*, 44–53.

(24) Azab, S. S.; Ashmawy, A. M.; Eldahshan, O. A. *Br. J. Pharm. Res.* **2013**, *3*, 78–89.

(25) Payghami, N.; Jamili, S.; Rustaiyan, A.; Saeidnia, S.; Nikan, M.; Gohari, A. R. *Pharmacogn. Res.* **2014**, *7*, 314–321.

(26) Uyanır, E.; Šoral, M.; Seyhan, G.; Akkaya, D.; Barut, B.; Sari, S.; Duman, H.; Renda, G.; Şöhretoğlu, D. *Chem. Biodivers.* **2024**, *21*, e202401386.

(27) Kitchen, D. B.; Decornez, H.; Furr, J. R.; Bajorath, J. *Nat. Rev. Drug Discov.* **2004**, 3, 935–949.

Received September 29, 2025
Revised January 17, 2026
Accepted March 5, 2026